Hydrochemical characteristics and water quality evaluation of shallow groundwater in Suxian mining area, Huaibei coalfield, China

Hao Yu[1,2] · Herong Gui[2] · Honghai Zhao[3] · Meichen Wang[1,2] · Jun Li[4] · Hongxia Fang[1,2] · Yaqi Jiang[1,2] · Yaru Zhang[2]

Abstract The aim of this study is to evaluate the hydrogeochemical characteristics and water environmental quality of shallow groundwater in the Suxian mining area of Huaibei coalfield, China. The natural formation process of shallow groundwater in Suxian is explored using Piper trilinear charts and Gibbs diagrams, and by examining the ratios between the major ions. United States Salinity Laboratory (USSL) charts, Wilcox diagrams, and the water quality index (WQI) are further employed to quantify the differences in water quality. The results reveal that the main hydrochemical facies of groundwater are HCO_3–Ca, and that silicate dissolution is the main factor controlling the ion content in shallow groundwater. The USSL charts and Wilcox diagrams show that most of the water samples would be acceptable for use in irrigation systems. The WQI results for each water sample are compared and analyzed, and the quality of groundwater samples around collapse ponds is found to be relatively poor.

1 Introduction

Groundwater resources are very valuable, and are indispensable for human and agricultural development (Aksoy and Scheytt 2007). More than 1.5 billion people worldwide rely on groundwater for domestic water (Adimalla and Qian 2019); in areas of limited precipitation and surface water resources, groundwater resources are particularly precious. Poor water quality not only poses a threat to human life and health, but also affects the growth of plants and animals (Zhang et al. 2012). Therefore, it is important to clarify the main factors affecting groundwater quality and water conditions (Sunkari et al. 2019). The Suxian mining area of Huaibei coalfield is a huge area of coal and grain production in China (Huang et al. 2018). The shallow groundwater in the area is often used in daily life (Chen et al. 2008; Qiu et al. 2018), but the wastewater discharged from the mine to the ground in the process of coal mining has the potential to pollute this water source (Lin et al. 2016; Ma and Gui 2017; Xiang et al. 2018) and have an adverse effect on the groundwater aquatic environment (Tahmasebi et al. 2018).

In recent years, the quality of groundwater has become an area of widespread concern for environmental workers. Khanoranga and Khalid (2019) used multivariate statistical analysis to study the groundwater around Balochistan, Pakistan, and found that natural factors and human activities are the main influences on groundwater chemical changes. Xu et al. (2019) studied the water environment

✉ Herong Gui
   guiherong@163.com

1 School of Earth and Environment, Anhui University of Science and Technology, Huainan 232001, Anhui, China

2 National Engineering Research Center of Coal Mine Water Hazard Controlling (Suzhou University), Suzhou 234000, Anhui, China

3 Anhui Provincial Bureau of Coal Geology Hydrologic Exploration Team, Suzhou 234000, Anhui, China

4 School of Resources and Environmental Engineering of Hefei University of Technology, Hefei 232000, Anhui, China

characteristics of the Guanzhong region in the north of China, while Lyu et al. (2019) investigated the Dakhu Basin in Northwest China and comprehensively studied the evolution characteristics and laws of groundwater using mathematical statistics and hydrogeological theory. This paper reports the results of a study focusing on the Suxian mining area in Huaibei coalfield. Analysis of shallow groundwater samples and data processing clarifies the hydrochemical characteristics and influential factors in this area, allowing the suitability of shallow groundwater as irrigation water to be determined. The evaluation provides a reference for the protection and scientific development of shallow groundwater in mining areas.

2 Study area

Huaibei coalfield and the Suxian mining area are situated in the southern part of Suzhou, Anhui Province, China. This region ranges from 116° 45′ E to 117° 12′ E, and from 33° 21′ N to 33° 42′ N (Fig. 1).

Covering an area of about 450 km², there are seven active coal mines in the research area: Zhou Zhuang, Qianyingyu, Qidong, Qinan, Luling, Zhuxianzhuang, and Taoyuan (Huang et al. 2017). The study area has four distinct seasons, with windy, cold winters and rainy, hot summers. The annual average temperature is 14.0–14.6 °C, with maximum temperatures reaching ∼ 40 °C and a minimum of − 12.5 °C. The annual rainfall is about 774–895 mm, and the annual evaporation is 832.4 mm. The diving resources are abundant, satisfying the demand for water in the research area (Gui and Chen 2015). In 2018, the grain crop planting area of Suzhou City covered 942,300 ha, the oil planting area covered 28,000 ha, the cotton planting area covered 0.21 million ha, the vegetable and edible fungus planting area covered 47,900 ha, and the annual grain output was 4.302 million tons.

In the study area, Cenozoic loose beds divide the groundwater into four aquifers, named, from top to bottom, the first, second, third, and fourth aquifers. Of these, the first aquifer (also known as "shallow groundwater") is the main research object in this paper. Its maximum thickness is about 30 m, and the water level is typically 1–3 m below the surface (Gui et al. 2015).

3 Materials and methods

3.1 Sample collection and analysis

Twenty-nine shallow groundwater samples were obtained from pumps (depths of less than 30 m) during March 2019. The location of each sampling point was recorded using

GPS. The electrical conductivity (EC), pH, and total dissolved solids (TDS) were measured immediately in the field using portable devices. The sampling bucket was cleaned three times with deionized water and sampled water samples before sampling. The water samples were sent to the laboratory within 8 h. Before testing, the water samples were filtered through a membrane with a pore-size of 0.45 μm. The major ions (Na^+, K^+, Ca^{2+}, Mg^{2+}, F^-, Cl^-, NO_3^-, and SO_4^{2-}) were then measured by ion chromatography (ICS-600-900), and the HCO_3^- ion concentration was determined by conventional acid–base neutralization titration.

3.2 Evaluation method

(1) Calculation of water quality index.

The water quality index (WQI) was used to assess the quality of shallow groundwater. WQI is an important tool in evaluating the overall quality of shallow groundwater, as it summarizes a large set of water quality data into a single value, enabling an effective understanding of the quality of shallow groundwater (Chen et al. 2019; Hou et al. 2016). WQI values have been used to study different water bodies and numerous results have been reported (Adimalla et al. 2018; Soleimani et al. 2018; Tiwari et al. 2017). WQI is calculated in four steps:

Step 1: Assign weights (w_i) to the water quality parameters (pH, EC, TDS, Na^+, K^+, Ca^{2+}, Mg^{2+}, F^-, Cl^-, NO_3^-, HCO_3^-, and SO_4^{2-}) according to their impact on water quality.
Step 2: Calculate the relative weight (W_i) of each parameter using the following equation:

$$W_i = \frac{w_i}{\sum_{i=1}^n w_i} \tag{1}$$

where W_i is the relative weight and w_i is the weight of the relevant water quality parameter.
Step 3: Calculate the quality level of each parameter using the following equation:

$$q_i = \frac{c_i}{s_i} \times 100 \tag{2}$$

where q_i is the quality level, c_i is the concentration measured for each parameter in mg/L, and s_i is the standard concentration set by the World Health Organization (WHO) for each parameter (see Table 1).
Step 4: Compute SI_i and WQI as:

$$SI_i = W_i \times q_i \tag{3}$$

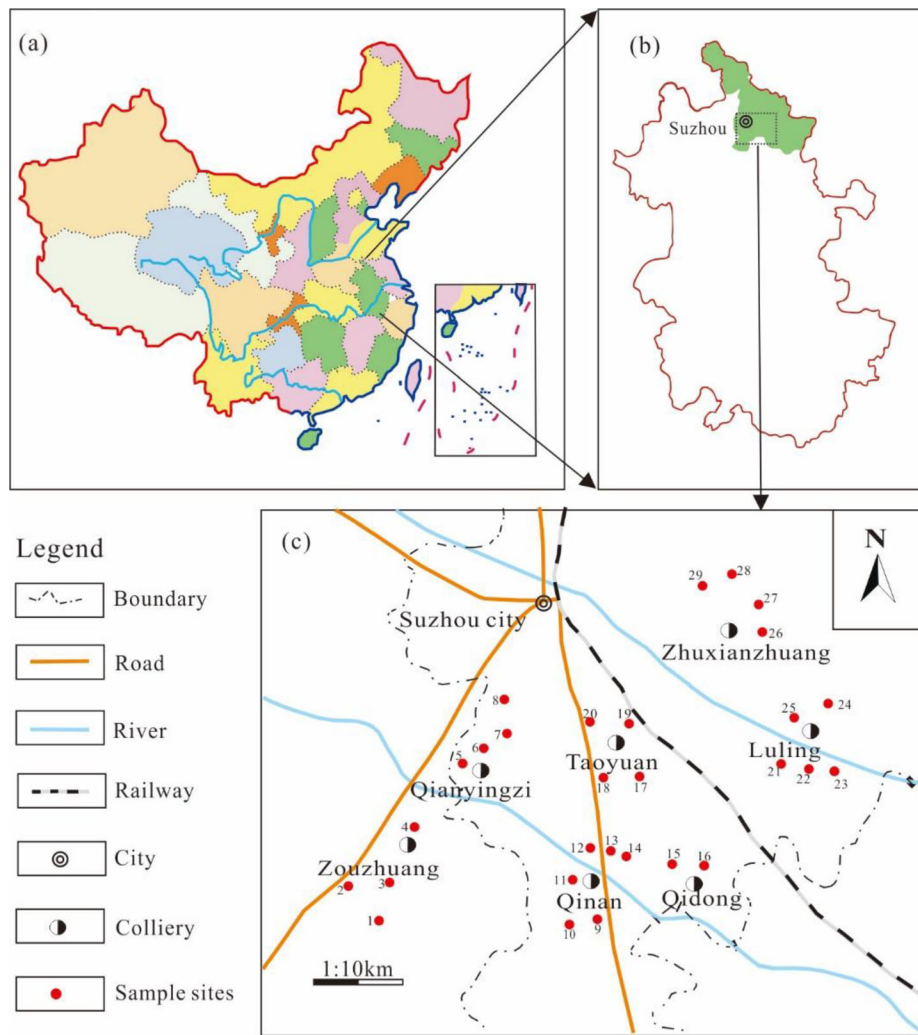$$WQI = \sum_{i=1}^n SI_i \tag{4}$$

Fig. 1 Study area and sampling locations

Table 1 Relative weights of the various shallow groundwater parameters

Parameter	WHO values (mg/L) (s_i)	Weight (mg)	Relative weight (mg)
pH	6.5–8.5	3	0.083
TDS	1000	5	0.139
K^+	12	2	0.056
Na^+	200	4	0.111
Ca^{2+}	200	3	0.083
Mg^{2+}	150	3	0.083
HCO_3^-	250	2	0.056
Cl^-	250	4	0.111
SO_4^{2-}	250	5	0.139
F^-	1.5	5	0.138

(2)   Irrigation quality evaluation of shallow groundwater

Groundwater is crucial for the irrigation of crops. If there is too much sodium in the irrigation water, the permeability of the soil will be reduced (Guan and Gui 2018) and the quality and yield of crops will be affected (Bob et al. 2016; Selvakumar et al. 2017a, b).

Therefore, it is vital to estimate the water quality of shallow groundwater used for irrigation: Sodium Adsorption Ratio (SAR), Residual Sodium Carbonate (RSC), Sodium Percentage (Na%), Permeability Index (PI), Magnesium Hazard (MH), Kelley's Ratio (KR), and *Potential Salinity* (PS). These indices are computed using the following equations:

$$Na\% = \frac{(Na^+ + K^+) \times 100}{Ca^{2+} + Mg^{2+} + Na^+ + K^+} \tag{5}$$

$$SAR = \frac{Na^+}{\sqrt{(Ca^{2+} + Mg^{2+})/2}} \tag{6}$$

$$RSC = (CO_3^{2-} + HCO_3^-) - (Ca^{2+} + Mg^{2+}) \tag{7}$$

$$MH = \frac{Mg^{2+}}{Ca^{2+} + Mg^{2+}} \times 100 \tag{8}$$

$$PI = \frac{Na^+ + \sqrt{HCO_3^-}}{Ca^{2+} + Mg^{2+} + Na^+ + K^+} \tag{9}$$

$$KR = \frac{Na^+}{Ca^{2+} + Mg^{2+}} \tag{10}$$

$$PS = Cl^- + \frac{1}{2}SO_4^{2-} \tag{11}$$

(The ion concentrations in Eqs. (5)–(11) are in units of meq/L.)

4 Results and discussion

4.1 Ion content statistics of groundwater

The statistical results for the hydrochemical parameters are presented in Table 2 alongside the WHO's drinking water quality standards (WHO 2011) and China's groundwater quality standards (GB/T 14848–2017). The pH ranges from 7.66 to 8.68, with an average of 8.17, which is slightly alkaline. According to the limits set by the WHO and China, the pH values of three samples are outside the allowable limits for drinking purposes, but are not at levels that would directly impact on human health (Cotruvo and Joseph 2017). The EC values vary from 500 to 1965 μS/cm, with a mean of 878.35 μS/cm. The results show that 27% of samples exceed the drinking water quality standards. Large changes in EC are usually caused by human

activities and geochemical processes (Adimalla and Qian 2019).

The concentrations of K^+ and Na^+ range from 0.23–0.81 mg/L and 17.83–290.44 mg/L, with average values of 0.47 mg/L and 75.57 mg/L, respectively. The Ca^{2+} and Mg^{2+} concentrations range from 22.87 to 167.95 mg/L and 17.31–82.30 mg/L, with average values of 55.27 and 34.79 mg/L, respectively. The cationic content of one water sample exceeds the WHO standards for drinking purposes (sodium concentration of 200 mg/L).

According to Fig. 2, the concentration of cations can be ranked as $Na^+ > Ca^{2+} > Mg^{2+}$, and that of anions runs as $HCO_3^- > SO_4^{2-} > Cl^-$.

The concentration of bicarbonate in the groundwater is affected by rock weathering and, to a lesser degree, atmospheric sources (Adimalla and Venkatayogi 2018). The values of HCO_3^- vary from 246.02–854.92 mg/L, with a mean of 470.39 mg/L. According to the WHO standards (WHO 2011), 96% of groundwater samples exceed the maximum allowable limit of 250 mg/L. The concentrations of Cl^- and SO_4^- anions vary from 3.60 to 195.55 mg/L and from 3.79 to 339.87 mg/L, with mean values of 36.58 and 37.98 mg/L, respectively. The results for SO_4^{2-} reveal that only one sample is outside the limit for drinking purposes.

Fluoride (F) is a basic trace element in the human body, but using high-fluorine drinking water over long periods can lead to chronic fluorine poisoning (Wu et al. 2018). The F values range from 0.28 to 1.86 mg/L, with a mean value of 1.11 mg/L. The majority of samples are below the permissible maximum set by the WHO (1.5 mg/L), while 38% of samples have double the permissible limit set by China (1.0 mg/L).

Higher values of NO_3-N are often found in agricultural regions of the world, a result of excessive use of fertilizers containing nitrogen (Adimalla 2018). The concentrations of NO_3-N range from 0.00 to 28.76 mg/L (mean value of 3.5 mg/L), with three water samples exceeding the permissible limit (10 mg/L).

4.2 Hydrochemical facies

Piper diagrams are widely used to investigate and classify the hydrogeochemical composition of groundwater (Xia et al. 2018). As shown in Fig. 3, the majority of water samples are in zone 5, which suggests that the predominant water type is HCO_3-Ca. It can be seen from Fig. 3 that there are two number of region 9, so a total of five water sample points fall in region 9, which took the second place was a mixed type. Only two samples fall in zone 8, both of which belonging to the type of HCO_3-Na. As seen from the distribute of cations, groundwater samples are divided into Ca type, Na type, and mixed type, which suggests the

Table 2 Statistical analyses of water quality parameters

Parameter	Unit	Maximum value	Minimum value	Mean value	SD	a	b	C*
pH	–	8.68	7.66	8.17	0.24	6.5–8.5	6.5–8.5	3
EC	μS/cm	1965.00	500.00	878.35	371.56	1000	–	8
TDS	mg/L	485.00	109.00	212.73	91.43	1000	1000	0
K^+	mg/L	0.81	0.23	0.47	0.12	12	–	0
Na^+	mg/L	290.44	17.83	75.57	60.47	200	–	1
Ca^{2+}	mg/L	167.95	22.87	55.27	32.76	200	–	0
Mg^{2+}	mg/L	82.30	17.31	34.79	15.84	150	–	0
HCO_3^-	mg/L	854.92	246.02	470.39	143.79	250	–	28
Cl^-	mg/L	195.55	3.60	36.58	47.56	250	250	0
SO_4^{2-}	mg/L	339.87	3.79	37.98	63.43	250	250	1
F^-	mg/L	1.86	0.28	1.11	0.42	1.5	1.0	4[a],18[b]
NO_3^--N	mg/L	28.76	0.00	3.50	6.70	10	10	3

Note: a-WHO guideline; b-Chinese guideline; C*-number of samples beyond limits; SD-standard deviation
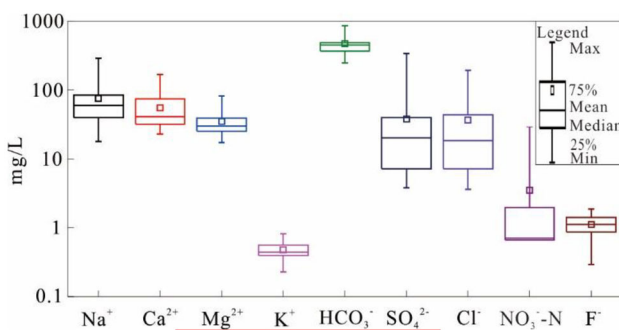
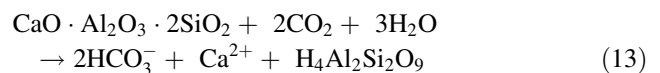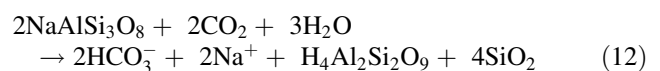**Fig. 2** Box diagram of different ions

groundwater type of the study area effect by ion exchange and weathering of silicate (Talib et al. 2019). With respect to anions, about 96% groundwater samples are belonging to bicarbonate type, and no points fall in zone F and G, which suggests that weathering of carbonate minerals is the key influencing factors for the groundwater hydrogeochemical compositions, and the dissolution of gypsum and evaporite is the secondary factor.

4.3 Natural formative process

To better understand the water chemical formation mechanism, Gibbs diagrams have been used to study the chemical composition of the world's surface water (Gibbs 1970). A Gibbs diagram consists of three parts, namely rock weathering, evaporation, and precipitation. As shown in Fig. 4, the majority of samples belong to the area dominated by rock weathering, which implies the groundwater chemical compositions are mainly influenced by rock weathering. In Fig. 4b, 55.2% of the groundwater

samples have $Na^+/(Na^++Ca^{2+})$ ratios greater than 0.5, which is indicative of ion exchange.

Figure 5 suggests that the groundwater samples mainly fall within the control area of silicate weathering, which further indicates that the hydrochemical formation of shallow groundwater in the study area is mainly affected by the dissolution of silicates according to:

$$2NaAlSi_3O_8 + 2CO_2 + 3H_2O \\ \rightarrow 2HCO_3^- + 2Na^+ + H_4Al_2Si_2O_9 + 4SiO_2 \quad (12)$$

$$CaO \cdot Al_2O_3 \cdot 2SiO_2 + 2CO_2 + 3H_2O \\ \rightarrow 2HCO_3^- + Ca^{2+} + H_4Al_2Si_2O_9 \quad (13)$$

4.4 Sources of major ions

The source of ions can be illustrated by plotting the proportional relationship of the major ions (Guan and Gui 2018). If the concentration of Na^+ and Cl^- came from halite (NaCl) (Talib et al. 2019), the ratio of Na^+/Cl^- would be close to 1.0. From Fig. 6a, it is apparent that most samples are distributed above the 1:1 line, which indicates the complexity of the Na^+ sources (Marghade et al. 2011), and suggests minerals with high Na^+ content, such as albite.

The ratio $(Ca^{2+}+Mg^{2+})/(SO_4^{2-}+HCO_3^-)$ reflects the dissolution degree of carbonates and sulfates. In Fig. 6b, most groundwater samples are below the 1:1 line. The samples below and above this diagonal are due to silicate and cation exchange (Guan and Gui 2018) and reverse cation exchange (Xu et al. 2019), respectively.

According to Fig. 6c, most samples fall in the range between the 1:1 and 2:1 lines, meaning that the main process is the dissolution of calcite and dolomite (Li et al. 2014). Only six samples lie above the 1:1 line, which
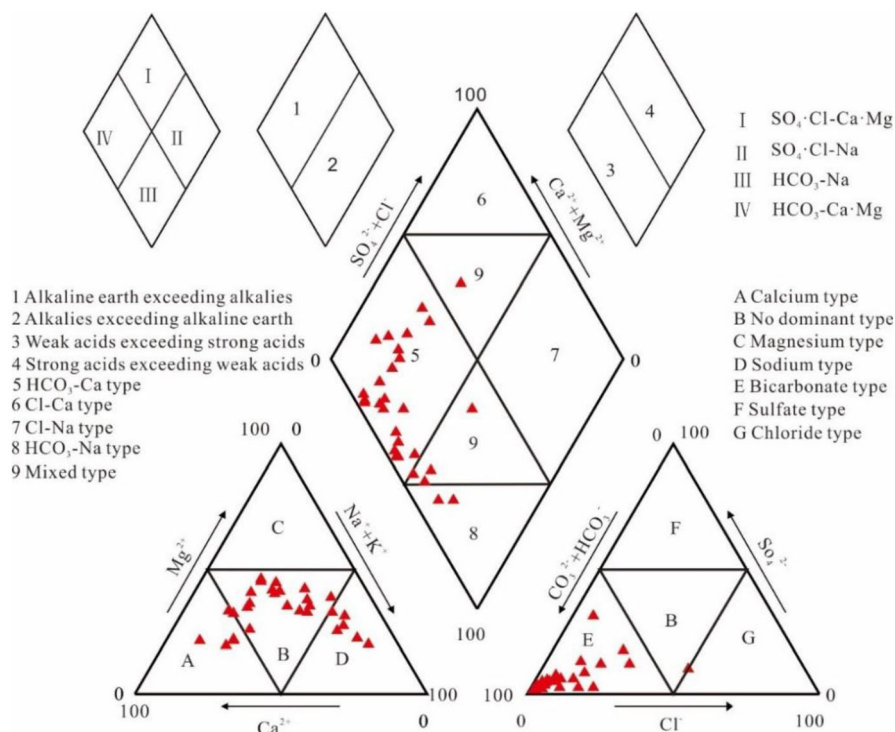
Fig. 3 Piper diagram

indicates the influence of gypsum dissolution. The ratio of $(Ca^{2+} + Mg^{2+}) - (SO_4^{2-} + HCO_3^-)$ to $Na^+ + K^+ - Cl^-$ is often used to verify the ion exchange (Xu et al. 2019). Figure 6d shows the linear relation between $(Ca^{2+} + Mg^{2+}) - (SO_4^{2-} + HCO_3^-)$ and $Na^+ + K^+ - Cl^-$. The fitting slope is -1.112, indicating the existence of cation exchange.

4.5 Assessment of groundwater quality using WQI

The WQI value was calculated according to the WHO drinking water quality standards (WHO 2011). According to the WQI values, the groundwater quality can be divided into three categories: good (< 50), poor (> 50), and very poor (> 75). When the WQI value > 100, it is not suitable for drinking (Talib et al. 2019). In this study, the WQI values of shallow groundwater calculated using Eqs. (1)–(4) range from 30.87–87.75. As shown in Fig. 7, 21 water samples (accounting for 72.4%) are of good quality, eight water samples (accounting for 24%) are of poor quality, and one sample is of very poor quality.

Water samples 20–24 were taken from the area surrounding Luling mine. Due to the long lifetime of this mine (more than 50 years), a large surface subsidence zone has formed. The subsidence area may have hydraulic contact with the surrounding shallow groundwater, and thus the groundwater quality is relatively poor.

Because shallow groundwater is fairly close to the surface, it is replenished by atmospheric rainfall and surface runoff. It is also vulnerable to pollution by domestic sewage, which may be the reason for the poor water quality of samples 7 (Qianyingzi Mine), 8 (Qianyingzi Mine), and 28 (Zhuxianzhuang Mine).

4.6 Groundwater suitability for irrigation

Suxian mining area is an important region of grain production in the northeast of Anhui Province. As most irrigation water is taken from the shallow groundwater, it is necessary to evaluate the water quality of shallow groundwater used as irrigation water. The quality of irrigation water is typically evaluated using United States Salinity Laboratory (USSL) charts (Richards 1954) and Wilcox charts (Wilcox 2002), as well as some single indicators. Equations (5)–(11) were used to calculate the relevant parameters, and the results are presented in Table 3. The SAR values, which reflect the degree of substitution of sodium for magnesium and calcium in soil (USDA 1954), suggest the extent of the impact on crops (Chen et al. 2019), with the SAR value < 18 indicating suitability for irrigation and $18 < SAR \leq 26$ indicating water that is unsuitable for irrigation for most types of soil. If the SAR value exceeds 26, the water is unsuitable for irrigation and has a very high sodium hazard. As show in
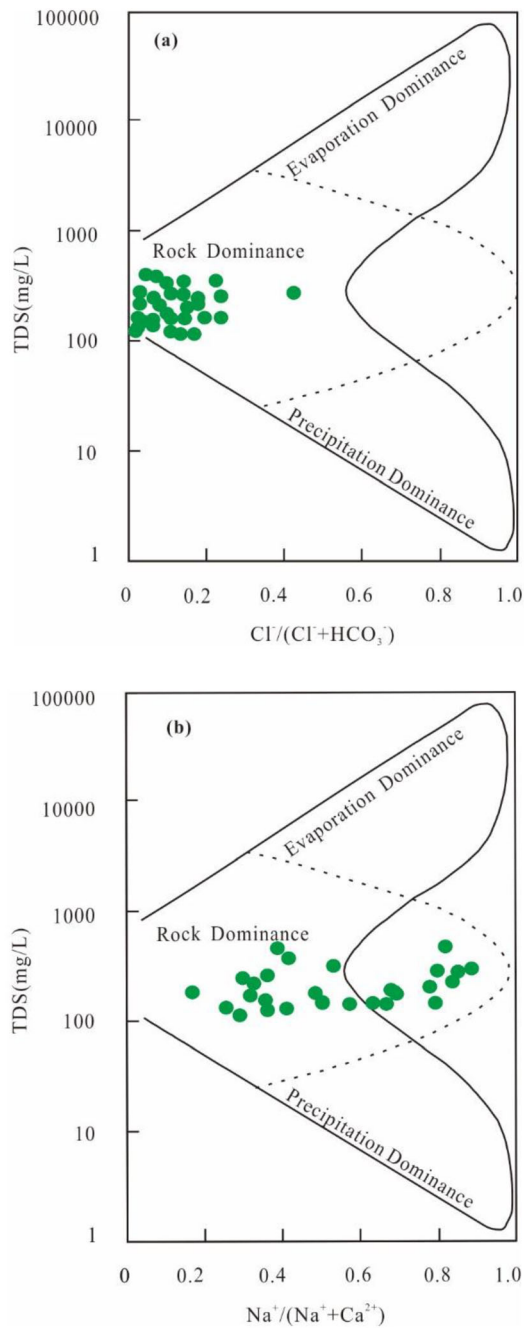
Fig. 4 Gibbs diagrams indicating the natural evolution mechanisms of groundwater

Fig. 5 Plot of **a** Na-normalized Ca^{2+} versus HCO_3^-; **b** Na-normalized Ca^{2+} versus Mg^{2+}

Table 3, the SAR values range from 0.45 to 6.28, with an average of 2.01.

Irrigation water with high electrical conductivity can lead to soil salinization. According to the EC values, the irrigation water body can be divided into areas C1 (low salinization, EC < 250 μS/cm), C2 (medium salinization, 250–750 μS/cm), C3 (high salinization, 750–2250 μS/cm), and C4 (highly salinized, EC > 2250 μS/cm). The USSL map combines the effects of SAR and EC on the soil. As

shown in the Fig. 8a, 15 water samples (51.72%) fall within area C2S1 for irrigation, while 13 water samples (44.83%) fall into the high-salt C3S1 area. If the soil leaching conditions are good, the shallow groundwater in these areas can be used for irrigation. Notably, only two water samples fall into area C3S2, which indicates high salt damage and medium alkali damage; such water is only suitable for the irrigation of plants with strong salt tolerance.

The percentage sodium is an important indicator of sodium risk. Higher Na% values may affect the structure of the soil, reduce its permeability, harden the soil body, and block the exchange of gas between the soil and the atmosphere. In this study, the Na% values were found to be between 11.63% and 69.70%, with an average of 34.11%. In general, when the Na% value of water exceeds 60%, it is not suitable for irrigation. Table 3 shows that only two shallow groundwater samples from the study area have Na% values above 60%. The Wilcox diagram combines the effect of Na% and EC on soil and plants. According to Fig. 8b, 15 water samples (51.72%) are in the "excellent" area, 10 water samples (43.48%) are in the "permissible" area, and only four samples belong to the "doubtful" area in which irrigation may lead to salinity damage. The overall water quality is therefore suitable for irrigation. If the MH value is less than 50, the water is suitable for irrigation. As shown in Table 3, about 31.03% of the samples are suitable for irrigation in terms of MH. In
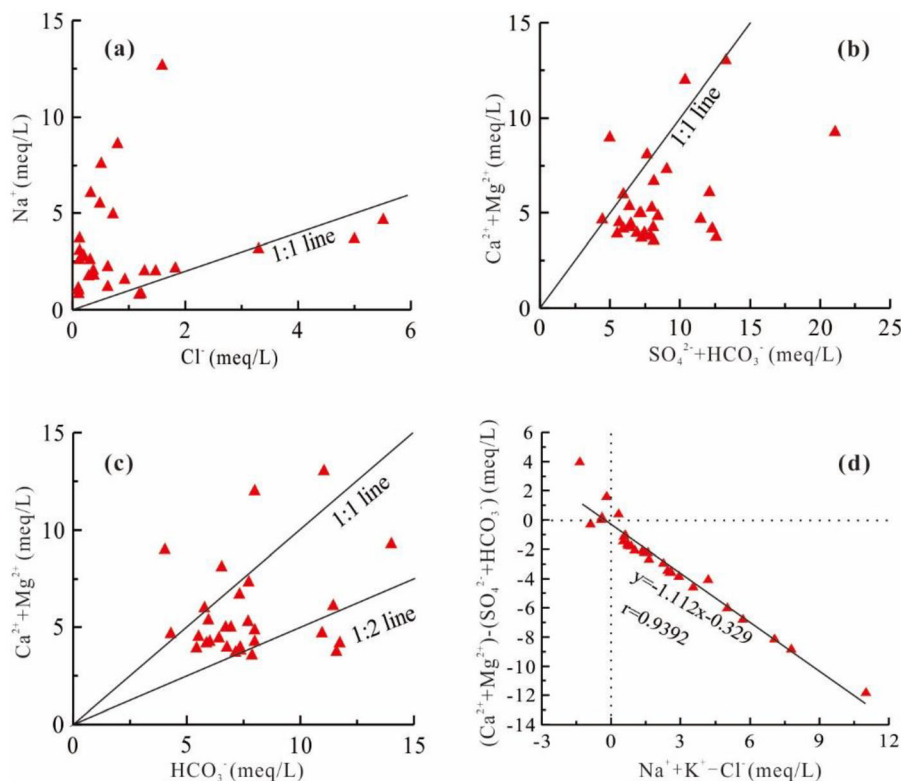
Fig. 6 Proportion diagrams of major ionic concentrations in the groundwater samples. **a** Na^+ versus Cl^-, **b** $Ca^{2+} + Mg^{2+}$ versus $SO_4^{2-} + HCO_3^-$, **c** $Ca^{2+} + Mg^{2+}$ versus HCO_3^-, **d** $(Ca^{2+} + Mg^{2+}) - (SO_4^{2-} + HCO_3^-)$ versus $Na^+ + K^+ - Cl^-$
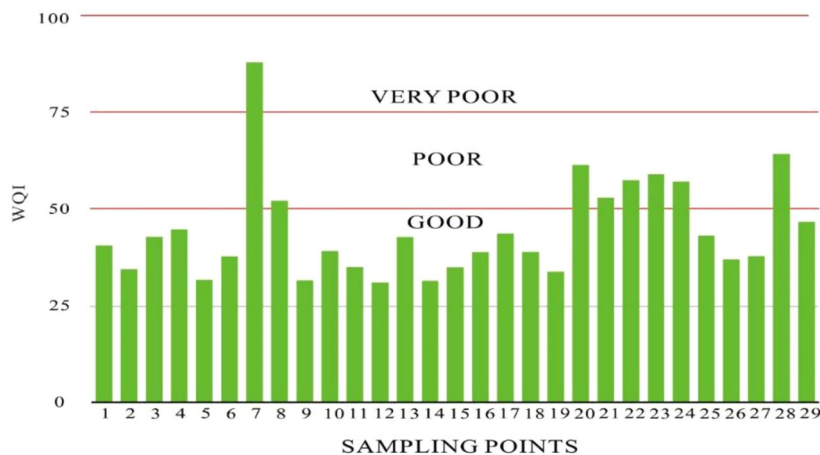

Fig. 7 WQI values

addition, the permeability index is an important parameter for evaluating the quality of irrigation water (Doneen 1964). As shown in Table 3, all PI values are acceptable for irrigation. Kelly's parameter (Kelly 1963) can also be used to evaluate irrigation water quality. Table 3 indicates that the KR values of shallow groundwater in the study area range from 0.13–2.30 (average 0.63), with five water samples exceeding the limit value. PS reflects the influence of chloride and sulfate concentrations on irrigation water quality (Doneen 1954). The PS values of all water samples are less than 10, indicating suitability for irrigation.

5 Conclusions

(1)　Suxian mining area is an important coal production base in the Huaibei coalfield. Large-scale coal

Table 3 Irrigation quality indices

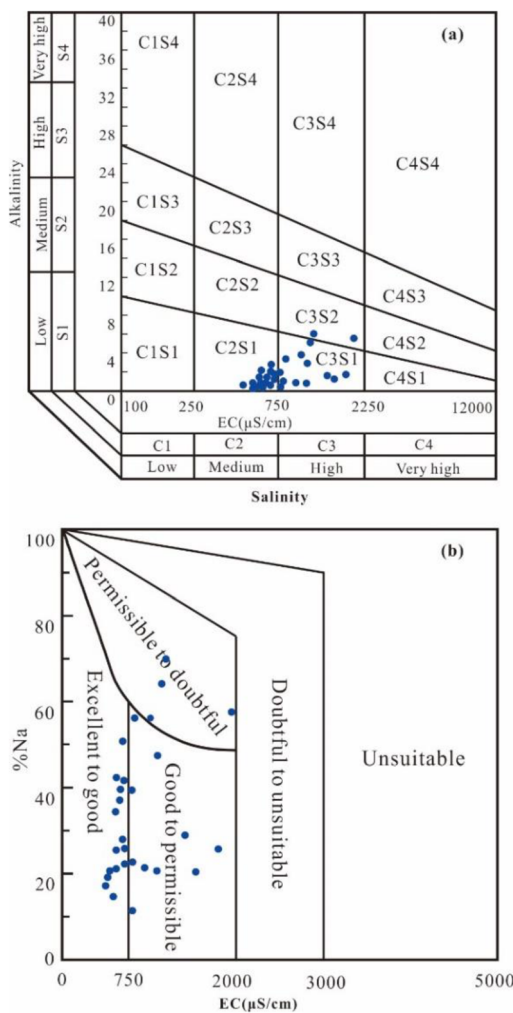| Index	Minimum value	Maximum value	Mean value	SD	Permissible limit	Number of unsuitable samples	Percent of suitable samples (%)
SAR	0.45	6.28	2.01	1.58	≤ 18	–	100
Na%	11.63	69.70	34.11	15.97	≤ 60	2	93.10
RSC	-4.91	7.85	2.05	2.98	≤ 2.5	12	58.62
MH	24.18	73.53	52.64	14.15	≤ 50	20	31.03
PI	39.42	97.28	68.11	16.13	≥ 25	–	100
KR	0.13	2.30	0.63	0.53	≤ 1.0	5	82.75
PS	0.14	6.63	1.43	1.75	≤ 10	–	100

Fig. 8 **a** USSL diagram and **b** Wilcox diagram

mining activities and domestic sewage discharge affect the quality of shallow groundwater. Therefore, analysis and evaluation of shallow groundwater in the study area is required to provide a reference for the protection and scientific development of shallow groundwater resources in the mining area.

(2) Shallow groundwater in the Suxian mining area is weakly alkaline. The main cation content is $Na^+ > Ca^{2+} > Mg^{2+}$ and the main anion content is $HCO_3^- > SO_4^{2-} > Cl^-$; the hydrochemical types are HCO_3–Ca and HCO_3–Na. Silicate dissolution and cation exchange are important factors controlling the ion composition of shallow groundwater in the study area; rock salt dissolution is not the only factor determining the content of sodium ions, as these may also come from minerals with high sodium contents, such as albite dissolution. The dissolution of gypsum, dolomite, and calcite is the main source of calcium and magnesium ions.

(3) Some water samples may be affected by surface subsidence areas formed by coal mining activities and domestic sewage, resulting in relatively poor water quality. The evaluation results of irrigation water quality showed that 51.72% of the shallow groundwater samples could be used for agricultural irrigation without causing salt or alkali damage; high salt damage was likely to occur from 44.83% of the water samples, which could be used for irrigation under better soil leaching conditions.

References

Adimalla N (2018) Groundwater quality for drinking and irrigation purposes and potential health risks assessment: a case study from semi-arid region of South India. Expo Health 11(2):109–123

Adimalla N, Qian H (2019) Groundwater quality evaluation using water quality index (WQI) for drinking purposes and human health risk (HHR) assessment in an agricultural region of Nanganur, south India. Ecotoxicol Environ Saf 176:153–161

Adimalla N, Venkatayogi S (2018) Geochemical characterization and evaluation of groundwater suitability for domestic and agricultural utility in semi-arid region of Basara, Telangana state, south India. Appl Water Sci 8(1):44

Adimalla N, Li P, Venkatayogi S (2018) Hydrogeochemical evaluation of groundwater quality for drinking and irrigation purposes and integrated interpretation with water quality index studies. Environ Process 5(2):363–383

Aksoy AO, Scheytt T (2007) Assessment of groundwater pollution around Torbali, Izmir, Turkey. Environ Geol 53(1):19–25

Bob M, Abd Rahman N, Elamin A, Taher S (2016) Assessment of groundwater suitability for irrigation in Madinah City, Saudi Arabia. Arab J Geosci 9(1):1–11

Chen LW, Gui HR, Yin XX (2008) Composing characteristic of hydrogen and oxygen stable isotopes and tracing of hydrological cycle. J China Coal Soc 10:1107–1111

Chen J, Huang Q, Lin Y, Fang Y, Qian H, Liu R, Ma H (2019) Hydrogeochemical characteristics and quality assessment of groundwater in an irrigated region, Northwest China. Water (Switzerland) 11(1):1–18

Cotruvo, Joseph A (2017) WHO guidelines for drinking water quality: first addendum to the fourth edition. J Am Water Works Assoc 109:44–51

Doneen LD (1954) Salination of soil by salts in the irrigation water. Eos Trans Am Geophys Union 35:943–950

Doneen LD (1964) Notes on water quality in agriculture. Water Science and Engineering Paper 4001, Department of Water Science and Engineering, University of California

Gibbs RJ (1970) Mechanisms controlling world water chemistry. Science 170(3962):1088–1090

Guan LS, Gui HR (2018) Hydrochemical characteristics and water quality assessment in goaf water of KouQuanGou mining area in Datong, Shanxi, China. Fresenius Environ Bull 27(12A):9315–9324

Gui HR, Chen S (2015) Isotopic geochemical characteristics of groundwater and its geological significance in Sunan mining area. Earth Sci Front 23(03):133–139

Gui HR, Chen LW, Song XM, Tu M, Qin Y, Ma J, Lin ML, Chen S, Peng WH, Liu XH, Li ZC, Liu X, Wang X (2015) Research on water-proof and sand-proof technology for coal-mining in the shallow structure of thick loose-bed overlying area. China University of Mining and Technology Press, Beijing

Hou W, Sun S, Wang M, Li X, Zhang N, Xin X, Jia R (2016) Assessing water quality of five typical reservoirs in lower reaches of Yellow River, China: using a water quality index method. Ecol Indic 61:309–316

Huang DW, Gui HR, Lin ML, Peng WH (2017) Accumulation characteristics and health risk of heavy metals in soil and plant: a case study from Huaibei Coalfield, China. Fresenius Environ Bull 26:8246–8254

Huang DW, Gui HR, Lin ML, Peng WH (2018) Chemical speciation distribution characteristics and ecological risk assessment of

heavy metals in soil from Sunan mining area, Anhui Province, China. Hum Ecol Risk Assess 24(6):1694–1709

Kelly W (1963) Use of saline irrigation water. Soil Sci 95:355–391

Khanoranga, Khalid S (2019) An assessment of groundwater quality for irrigation and drinking purposes around brick kilns in three districts of Balochistan province, Pakistan, through water quality index and multivariate statistical approaches. J Geochem Explor 197:14–26

Li P, Wu J, Qian H, Lyu X, Liu H (2014) Origin and assessment of groundwater pollution and associated health risk: a case study in an industrial park, northwest China. Environ Geochem Health 36(4):693–712

Lin ML, Peng WH, Gui HR (2016) Hydrochemical characteristics and quality assessment of deep groundwater from the coal-bearing aquifer of the Linhuan coal-mining district, northern Anhui province, China. J Environ Monit Assess 188(4):202

Lyu M, Pang Z, Huang T, Yin L (2019) Hydrogeochemical evolution and groundwater quality assessment in the Dake Lake Basin, Northwest China. J Radioanal Nucl Chem 320(3):865–883

Ma L, Gui HR (2017) Characteristics and source identification of heavy metals in subsidence Lake in Zhuxianzhuang coal mine in the north of Anhui Province, China. Earth Environ 45(3):277–282

Marghade D, Malpe DB, Zade AB (2011) Geochemical characterization of groundwater from northeastern part of Nagpur urban, Central India. Environ Earth Sci 62(7):1419–1430

Qiu HI, Gui HR, Song QX (2018) Human health risk assessment of trace elements in shallow groundwater of the Linhuan coal-mining district, Northern Anhui Province, China. J Hum Ecol Risk Assess 24(5):1342–1351

Selvakumar S, Chandrasekar N, Kumar G (2017a) Hydrogeochemical characteristics and groundwater contamination in the rapid urban development areas of Coimbatore, India. Water Resour Ind 17:26–33

Selvakumar S, Ramkumar K, Chandrasekar N, Magesh NS, Kaliraj S (2017b) Groundwater quality and its suitability for drinking and irrigational use in the Southern Tiruchirappalli district, Tamil Nadu, India. Appl Water Sci 7(1):411–420

Soleimani H, Nasri O, Ojaghi B, Pasalari H, Hosseini M, Hashemzadeh B, Feizabadi GK (2018) Data on drinking water quality using water quality index (WQI) and assessment of groundwater quality for irrigation purposes in Qorveh & Dehgolan, Kurdistan, Iran. Data Brief 20:375–386

Sunkari ED, Abu M, Bayowobie PS, Dokuz UE (2019) Hydrogeochemical appraisal of groundwater quality in the Ga West municipality, Ghana: implication for domestic and irrigation purposes. J Groundw Sustain Dev 8:501–511

Tahmasebi P, Mahmud-Gharaie MH, Ghassemzadeh F, Karouyeh AK (2018) Assessment of groundwater suitability for irrigation in a gold mine surrounding area, Iran. Environ Earth Sci 77:766

Talib MA, Tang Z, Shahab A, Siddique J, Faheem M, Fatima M (2019) Hydrogeochemical characterization and suitability assessment of groundwater: a case study in central Sindh, Pakistan. Int J Environ Res Public Health 16(5):835

Tiwari AK, Ghione R, De Maio M, Lavy M (2017) Evaluation of hydrogeochemical processes and groundwater quality for suitability of drinking and irrigation purposes: a case study in the Aosta Valley region, Italy. Arab J Geosci 10(12):264

Richards LA (1954) Diagnosis and improvement of Saline and Alkali soils. USDA Handbook.Soil ence 78(2):154

Wilcox LV (2002) Classification and use of irrigation waters. Glycobiology 12(3):229–234

World Health Organization (2011) Guidelines for drinking-water quality, 4th edn

Wu C, Wu X, Qian C, Zhu G (2018) Hydrogeochemistry and groundwater quality assessment of high fluoride levels in the

Yanchi endorheic region, northwest China. Appl Geochem 98:404–417

Xia YT, Gui HR, Zhao HH, Li J, Guan LS (2018) Temporal variability of hydro-chemical characteristics and water quality assessment of collapse pond in Zhuxianzhuang coal mining area, China. Fresenius Environ Bull 28(1):402–409

Xiang L, Zheng LG, Cheng H (2018) Spatial variability in water quality and relationships with land use in a coal-mining subsidence area of China. Fresenius Environ Bull 27(7):4782–4788

Xu PP, Feng WW, Qian H, Zhang Q (2019) Hydrogeochemical characterization and irrigation quality assessment of shallow groundwater in the central-western Guanzhong Basin, China. Int J Environ Res Public Health 16(9):1492

Zhang B, Song X, Zhang Y, Han D, Tang C, Yu Y, Ma Y (2012) Hydrochemical characteristics and water quality assessment of surface water and groundwater in Songnen plain, Northeast China. Water Res 46(8):2737–2748